Jurnal Teknologi

Full Paper

COMPARATIVE ELECTROCHEMICAL BEHAVIOUR ANALYSIS OF IRON-BASED ELECTRODES FOR AR18 DYE REMOVAL VIA ELECTROCOAGULATION

Nurulhuda Amri[a]*, Ahmad Zuhairi Abdullah[b], Mohamad Sabri Mohamad Sidik[c]

[a]Chemical Engineering Studies, Universiti Teknologi MARA, Cawangan Pulau Pinang, 13500 Permatang Pauh, Pulau Pinang, Malaysia
[b]School of Chemical Engineering, Universiti Sains Malaysia, Engineering Campus, 14300 Nibong Tebal, Penang, Malaysia
[c]Malaysian Spanish Institute, Universiti Kuala Lumpur, 09000 Kulim, Kedah, Malaysia

Article history
Received
12 September 2023
Received in revised form
2 March 2025
Accepted
7 March 2025
Published Online
24 October 2025

*Corresponding author
nurulhuda.amri@uitm.edu.my

Graphical abstract

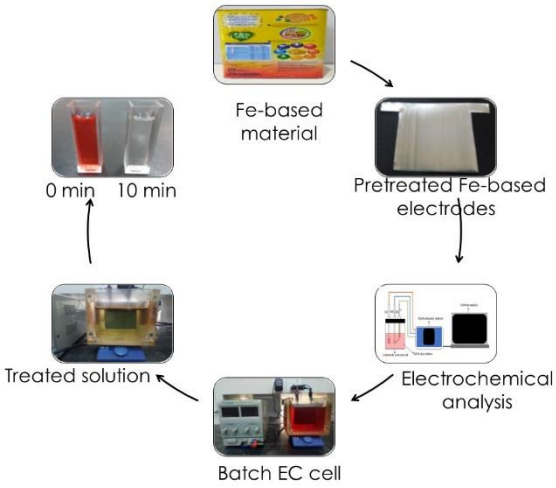

Abstract

The electrocoagulation (EC) process has emerged as a viable alternative for treating textile effluent before its release into the environment. However, a notable limitation of this method is the requirement for frequent replacement of the sacrificial anode, leading to elevated costs associated with electrode material. Thus, this research aims to conduct a comparative study between waste steel containers (WSC) and commercially available iron (Fe) electrodes in terms of electrochemical behaviour that significantly influences the EC performance in treating Acid Red 18 (AR18) dye. The electrochemical experiments were performed using an electrochemical analyser, followed by a batch EC experiment for AR18 dye removal. The results indicate that the WSC electrode has a more negative corrosion potential, Ecorr value of -0.954 V vs. SCE, compared to Commercial Pure Iron (CPI) at -0.947 V vs. SCE and Commercial Mild Steel (CMS) at -0.908 V vs. SCE. This suggests that WSC is more susceptible to corrosion, leading to a higher dissolution rate of Fe ions than the commercial electrodes. The findings were also in line with the EC performance, where the removal efficiency of the WSC electrode (99.7%) was found to be slightly higher than that of the commercial electrodes of CMS (98.7%) and CPI (98.1%). In conclusion, the utilization of WSC has demonstrated its efficacy as an electrode option to serve as an alternative to conventional Fe electrodes in the treatment of AR18 dye solutions.

Keywords: AR18 dye removal, electrochemical behaviour, electrocoagulation, Fe-based electrodes

Abstrak

Proses elektrokoagulasi (EC) telah menjadi alternatif yang berdaya maju untuk rawatan air sisa tekstil sebelum dilepaskan ke alam sekitar. Walau bagaimanapun, kelemahan utama kaedah ini adalah keperluan untuk penggantian anod korban secara kerap, yang

membawa kepada peningkatan kos yang berkaitan dengan bahan elektrod. Oleh itu, penyelidikan ini bertujuan untuk menjalankan kajian perbandingan antara elektrod bekas sisa keluli (WSC) dan elektrod besi (Fe) komersial dari segi tingkah laku elektrokimia yang boleh mempengaruhi prestasi EC dalam rawatan penyingkiran pewarna merah asid 18 (AR18). Eksperimen elektrokimia dijalankan menggunakan penganalisis elektrokimia diikuti dengan eksperimen EC untuk penyingkiran pewarna AR18. Keputusan menunjukkan bahawa elektrod WSC mempunyai potensi kakisan, E_{corr} yang lebih negatif sebanyak -0.954 V vs SCE, berbanding besi tulen komersial (CPI) pada -0.947 V vs SCE dan keluli ringan komersial (CMS) pada -0.908 V vs SCE. Ini menunjukkan bahawa WSC lebih cenderung kepada kakisan, yang membawa kepada kadar pembubaran ion Fe yang lebih tinggi daripada elektrod komersial. Penemuan ini juga adalah selari dengan prestasi EC di mana kecekapan penyingkiran bagi elektrod WSC (99.7%) didapati lebih tinggi daripada elektrod komersial CMS (98.7%) dan CPI (98.1%). Kesimpulannya, penggunaan WSC sebagai alternatif kepada konvensional elektrod Fe telah menunjukkan keberkesanannya dalam rawatan penyingkiran pewarna AR18.

Kata kunci: Penyingkiran pewarna AR18, tingkah laku elektrokimia, elektrokoagulasi, elektrod berasaskan Fe

1.0 INTRODUCTION

For numerous decades, the textile industry in Malaysia has played a vital role in bolstering the nation's economy and providing substantial employment opportunities. However, this industry relies on a wide range of chemicals for processes like dyeing, bleaching, and finishing. Improper disposal of these chemicals can lead to soil and water contamination, affecting ecosystems and potentially harming human health. Azo dyes are commonly utilised in the textile industry because of their stability, low cost, resistance and ability to produce a variety of colours [1]. However, the azo group dyes pose a high risk to health, as toxic and carcinogenic amines are released by the chromophore's cleavage during the degradation reaction [2]. Acid red 18 (AR18) is an azo dye classified as anionic with two main absorbance bands in the visible region, located at the wavelength of 507 nm and 330 nm, corresponding to the chromophore containing azo linkage and aromatic (naphthalene) rings, respectively.

Electrocoagulation (EC) is an electrochemical process involving direct current and sacrificial anodes to produce metal coagulants without the use of chemical reagents. It is a potential technique for treating textile industrial effluent because of its simple design, ease of operation, and ability to effectively remove a wide range of pollutants [3, 4, 5]. The EC method depends on using electricity to produce coagulants from the electrodes. These coagulants help heavy particles settle in the water, while gas bubbles formed during the process aid in floating lighter constituents [6]. Thus, the EC method has the potential to simultaneously remove various contaminants like dyes, COD, heavy metals and suspended solids (TSS) from textile wastewater [7, 8, 9].

Electrode material selection is crucial because it not only influences the efficiency of the EC process but also plays a significant role in determining energy consumption and operational expenses. The most commonly used electrodes for the EC process are Al and Fe electrodes. Several studies have demonstrated the effectiveness of Al and Fe electrodes used in treating various types of dyes pollutant via the EC process [3, 10]. Recently, more research has highlighted the utilization of waste-based materials as sacrificial electrodes in the EC process. These materials include Fe anode scrap [11], food can waste [12] and Al plate scrap [13], Al and Fe scrap from industrial waste [14] and various types of metallic wastes, including beverage cans, used Al foil, scrap iron, and scrap mild steel [15]. Exploring waste materials as electrodes aims to reduce the high operational costs of regular electrode replacement in the EC process.

In this work, a waste steel container (WSC) is used as one of the sustainable alternatives to commercial Fe electrodes in the electrocoagulation (EC) process. In general, electrodes made of different Fe-based materials represent different compositions of metal elements and electrochemical behaviour that can significantly affect the rate of electrode dissolution as well as EC performance [16]. Bani-Melhem and Al-Kilani (2023) compared the efficiency of iron and mild steel electrodes in treating highly loaded grey water [17]. Their findings indicated that mild steel electrodes outperform iron electrodes in pollutant removal efficiency and energy consumption, likely due to differences in metal alloy composition or the physical

properties of the electrodes. In the other study, Dura & Breslin (2019) also reported on comparing the electrochemical behaviour of the Fe and stainless steel electrodes used in the EC process to remove Orange II dye, Zn^{2+} and phosphates simultaneously from synthetic wastewater [18]. They reported that the highest removal efficiencies of Orange II dye, Zn^{2+} and phosphates were obtained by pure Fe electrode, which has a more negative E_{corr} value and no passive film formation. To date, no study has been reported on the electrochemical behaviour of the WSC and its comparison with the commercial Fe electrodes as well as their EC performance for the removal of AR18 dye.

Thus, this research aimed to investigate the electrochemical behaviour of the WSC and the commercial Fe electrodes, which are commercial mild steel (CMS) and commercial pure iron (CPI), using potentiodynamic polarisation analysis via a three-electrode electrochemical system. The batch EC process at a constant current density of 25 mA/cm^2, initial AR18 dye concentration of 100 mg/L and pH of 6.8 was then conducted to investigate the correlation of the electrochemical behaviour of the three different Fe-based electrodes (WSC, CMS and CPI) with EC performance for AR18 dye removal.

2.0 METHODOLOGY

2.1 Materials

Waste steel container (WSC), commercial mild steel (CMS) and commercial pure iron (CPI) were chosen as Fe-based electrodes for the decolourisation of AR18 dye using the EC process. The waste steel container (WSC), a food tin packaging manufactured by Mondelez Malaysia Sdn. Bhd., was collected from student hostels at Universiti Sains Malaysia, as shown in Figure 1 (a). Meanwhile, both commercial electrodes, which are commercial mild steel (CMS) and commercial pure iron (CPI), were obtained from Neilement Engineering Resources & Services, Penang. The elemental compositions of the WSC are Fe (83.65%), C (9.98%), O (3.63%) and Sn (2.74%), which was determined using Energy-dispersive X-ray (EDX) analysis [19]. The CMS was categorized under a mild/low carbon steel with a composition of Fe (98.81-99.26% as remainder), C (0.14-0.20% max), Mn (0.60-0.90% max), P (< 0.04% max) and S (0.05% max) [20]. Meanwhile, CPI was a pure iron with a composition of 99.9% Fe.

The dimensions of the commercial electrodes were 7 cm x 6 cm x 0.1 cm (W x H x T), as illustrated in Figure 1 (b). The WSC was also cut into dimensions resembling commercial electrodes but with a different thickness of 0.03 cm (the original thickness of the WSC). They were then pre-treated with SiC paper (P180) to eliminate the decorative paint and chemical coatings from both the outer and inner walls of the metal waste. Meanwhile, the commercial electrodes were polished by sanding both sides of the electrodes with the same SiC paper, followed by rinsing with deionized water to remove any contaminants and oxides layer to activate the electrode's surface before being used in each of the EC experiments.

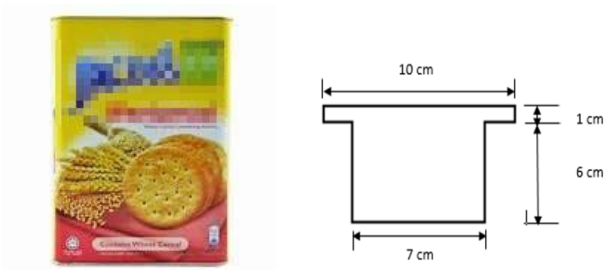

Figure 1 (a) Waste steel container (WSC) used as iron-based electrodes and (b) Dimensions of WSC electrode

2.2 Electrochemical Study for the Pre-treated Waste-Based and Commercial Electrodes

The electrochemical experiments were conducted using a compact electrochemical analyser (PalmSens4, Netherlands) connected to a computer with PSTrace 5.8 software. The schematic diagram of the electrochemical set-up for the three-electrode system is shown in Figure 2. The electrochemical measurements were performed using 80 mL of 100 mg/L AR18 dye solution with 2 g/L NaCl, at room temperature in a three-electrode standard corrosion cell with a volume of 100 mL. The working electrodes (WE), which were either pre-treated WSC, CMS or CPI, were embedded in a Teflon holder with an exposed area of 1.0 cm^2. A platinum electrode with a surface area of 2.0 cm^2 served as the counter electrode (CE), while a saturated calomel electrode (SCE) ($Hg/Hg_2Cl_2/KCl$) was positioned in a Luggin capillary to function as the reference electrode (RE) (E = 0.241 V versus standard hydrogen electrode). The surface area of the CE should be larger than the surface area of the WE to ensure that the kinetics of the reaction occurring at the CE did not inhibit those occurring at the WE.

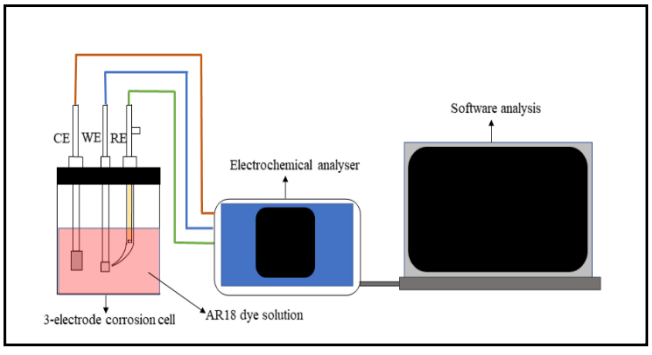

Figure 2 The schematic diagram of the electrochemical set-up for the three-electrode system

Before each of the analyses, the PalmSens instrument was calibrated using a dummy cell to ensure the reading was accurately recorded. Next, the open circuit potential (OCP) was performed for 30 minutes by monitoring the anode potential (V vs SCE) by time to ensure the stabilisation of the electrode was achieved before the potentiodynamic polarisation analysis [21]. The polarisation curves were then recorded, starting at −1.5 V vs. SCE up to 0.0 V SCE using a scan rate of 5 mV/s. The experiments were conducted a minimum of three times, and the measurement that best represented the results was chosen for plotting.

For large overpotentials, the Tafel equations for the anodic and cathodic reactions are given by Equation (1) and (2), respectively [22]. Accordingly, the Tafel plot was obtained by plotting the logarithm of the current density (log *j*) as a function of overpotential. The classical Tafel analysis was performed by extrapolating the anodic and cathodic Tafel lines. The corrosion current density, denoted as j_{corr}, was calculated by identifying the intersection point between the cathodic slope and a line passing through the corrosion potential, E_{corr}.

$$\text{Anodic reaction, } \eta = a + \beta_a \log j \quad (1)$$

$$\text{Cathodic reaction, } \eta = a' + \beta_c \log j \quad (2)$$

Where η is overpotential, a is anodic constant $\left(-\frac{2.303\,RT}{anF} \log j_0\right)$, a' is cathodic constant, $\left(\frac{2.303\,RT}{(1-a)nF} \log j_0\right)$, β_a is anodic Tafel slope, β_c is cathodic Tafel slope, j is measured current density, α is transfer coefficient, n is number of electrons, F is Faraday's constant (96,485 C/mol), R is universal gas constant (8.314 J/K.mol) and T is temperature (K).

The optical images of the electrode surface were recorded after polarisation experiments using a digital optical microscope (HD Colour CMOS Sensor, High-Speed DSP) with a magnification of 1600x and an optimum resolution of 640 x 480. This microscope was also equipped with digital measurement software and a calibration ruler.

2.3 Batch EC Process

Batch monopolar EC experiments were conducted in a rectangular EC cell reactor with a capacity of 1.1 L. Two pieces of Fe-based electrodes were used as electrodes and placed at the centre of the cell, with a 0.5cm gap between electrodes. Each electrode submerged in the solution had dimensions of 6 cm x 7 cm, providing a total effective surface area of 84 cm^2 for both sides of the anode. An 800 mL volume of the AR18 dye solution was initially introduced into the electrocoagulation (EC) cell. The electrodes were connected to an external DC power supply using crocodile wire clips to supply the required current to the system, as shown in Figure 3.

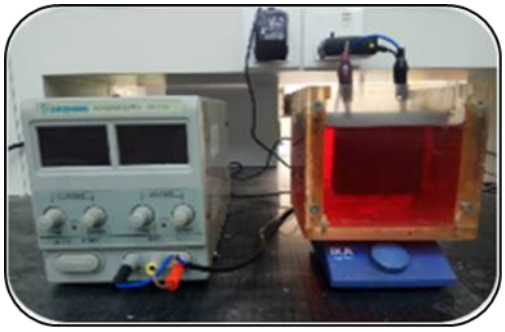

Figure 3 The experimental setup of the EC cell

Throughout the EC process, a magnetic stirrer (Topolino, IKA) was used to ensure continuous and uniform mixing of the solution at a medium speed. All experiments were conducted at a room temperature of 25±1 °C. The pH of the samples was assessed using a pH meter (Eutech pH2700, Thermo Scientific). Treated AR18 dye samples were collected at various time intervals and passed through Whatman filter paper before their concentrations were determined using a double-beam UV-visible spectrophotometer (UV-1800, Shimadzu, Japan) at the maximum wavelength, λ_{max} of 507 nm. The dye removal efficiency for each of the run is calculated using Equation (3):

$$\text{Removal Efficiency, \%} = \frac{C_0 - C_t}{C_0} \times 100\% \quad (3)$$

Where C_0 is initial dye concentration (mg/L) and C_t is dye concentration at a time, t (mg/L).

Each of the EC experiments was performed twice [23, 24, 25, 26] and the average dye removal efficiency was calculated to ensure the precision and consistency of the experimental data with variations within ±5% of standard deviation (SD). The SD value was determined using Eq. (4). The variations of the experimental data are represented by the error bars marked in the plotted graphs.

$$SD = \sqrt{\frac{1}{n-1}\sum_{i=1}^{n}(x_i - \bar{x})^2} \quad (4)$$

Where x_i is the dye removal efficiency (%), $\bar{x}$ is the average of dye removal efficiency (%) and n is the number of experimental data points.

The concentrations of Fe ions remaining in the treated water were then analysed using an inductively coupled plasma-optical emission spectrometer (ICP-OES) (ICAP 7600, Thermo Scientific, USA) using the APHA 3120 (B) standard method. The ICP analysis was carried out at a nebulizing argon flow of 0.50 L/min, a radio frequency generator power of 1,150W, a plasma gas flow rate of 12 L/min and an auxiliary gas flow rate of 0.50 L/min.

2.4 The Operational Cost

The operational cost is typically assessed by considering the energy, electrode, and chemical consumption utilized during the EC process. The electrode consumption cost for WSC in this present study was neglected since the electrodes used originated from waste material. However, the electrode consumption of the commercial electrodes was included in the overall operational cost. The electrical energy consumption (EEC), electrode consumption (ELC) and overall operating cost are calculated using Equation (5), Equation (6) and Equation (7), respectively [27]:

$$\text{EEC, } \left(\frac{\text{kWh}}{\text{m}^3}\right) = \frac{\text{V x I x t}}{1000 \text{ x v}} \quad (5)$$

Where V is applied voltage (V), I is required current (A), t is time (h) and v is volume of dye solution (m^3).

$$\text{ELC, } \left(\frac{\text{kg}}{\text{m}^3}\right) = \frac{\text{I x t x M}}{\text{z x F x v x 1000}} \quad (6)$$

Where I is required current (A), t is time (h), M is molecular mass of the Fe electrode (55.84 g/mol), *z* is number of electrons transferred (Z_{Fe}=2), F is Faraday constant (96,485 C/mol) and v is volume of dye solution (m^3).

Operating cost, (RM/m^3)= a x EEC +b x CC +c x ELC (7)

Where a is electricity price (RM/kWh), b is chemical unit price (RM/kg), c is material price (RM/kg), EEC is electrical energy consumption (kWh/m^3), CC is chemical consumption (kg/m^3) and ELC is electrode consumption (kg/m^3).

Based on the rates and tariffs in Malaysia throughout January 2021, the electrical cost was RM0.337/kWh as per the electricity rate for the industrial application [28]. Meanwhile, the metal price based on the London Metal Exchange for steel/Fe materials was RM3.49/kg [29]. The price for NaCl chemical was RM0.70/kg [30].

3.0 RESULTS AND DISCUSSION

3.1 Electrochemical Behaviour of Different Fe-Based Electrodes

The electrochemical study, including corrosion and passive behaviour, was compared between WSC, CMS and CPI electrodes using potentiodynamic polarisation analysis. The experimental runs for this electrochemical study were carried out in a 100 mg/L AR18 dye solution with 2 g/L NaCl as a supporting electrolyte. The potentiodynamic polarisation curves recorded for different Fe-based electrodes are illustrated in Figure 4, and the Tafel data obtained from the curve plots are tabulated in Table 1.

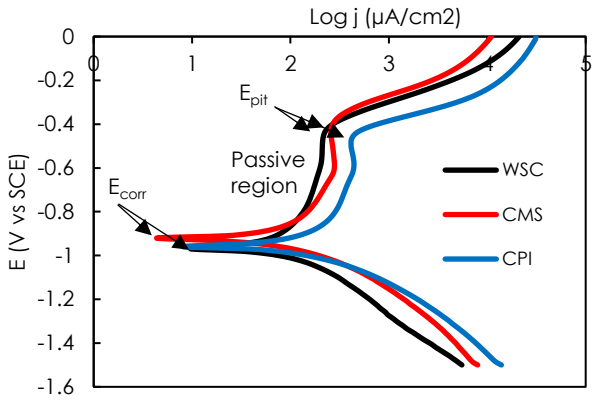

Figure 4 Effect of different Fe-based electrode materials on potentiodynamic polarisation curve. (AR18 dye initial concentration= 100 mg/L and NaCl = 2 g/L)

Table 1 Parameters obtained from the potentiodynamic polarisation test by the Tafel extrapolating method for different Fe-based electrodes

Parameters	WSC	CMS	CPI
E_{corr}, (V)	-0.954	-0.908	-0.947
j_{corr}, (μA/cm^2)	61.14	58.20	59.02

The corrosion potential, E_{corr} of WSC was found to be more negative value with -0.954 V vs. SCE than CPI and CMS electrodes with -0.947 V vs. SCE and -0.908 V vs. SCE, respectively. As expected, the j_{corr} value was consistent with the E_{corr} in which the highest j_{corr} value was represented by WSC (61.14 μA/cm^2) followed by CPI (59.02 μA/cm^2) and CMS (58.20 μA/cm^2) (Table 1). The more negative E_{corr} and higher j_{corr} for WSC indicate that WSC is more prone to corrosion and hence exhibits a higher dissolution rate of Fe ions compared to CPI and CMS. The finding was in agreement with the study reported by Dura & Breslin (2019) [18] and Sarah *et al.* (2024) [16]. This was attributed to the presence of a small amount of Sn remaining on the WSC surface after the pre-treatment, which resulted in galvanic corrosion [31].

Galvanic corrosion, also called bimetallic corrosion, occurs when two dissimilar metals are electrically connected in a conductive solution, resulting in an electrical potential difference [32]. In the case of WSC, the Sn on the WSC surface was more stable than the underlying steel. This means that Sn is less likely to corrode compared to the steel, leading to preferential corrosion of the steel when both are in electrical contact. This phenomenon caused WSC metal to corrode faster at an anode, which was corroborated by a more negative E_{corr} value than that of commercial Fe electrodes. However, at the potential level higher than E_{corr}, an intense passive region was remarkably more evident in WSC electrodes than in commercial ones, as illustrated in Figure 4. Thus, a slightly higher energy supply might be required by the EC system with the WSC electrode.

Meanwhile, a similar trend of active-passive transition, often referred to as an 'anodic nose", was demonstrated by both commercial electrodes of CMS and CPI. This transition was also reported for stainless steel alloys, such as AISI310 behaviour in 0.017 M NaCl [22].

Furthermore, a pitting attack was evidenced, with the distribution and size of the pits varying according to the type of Fe materials used (Figure 5).

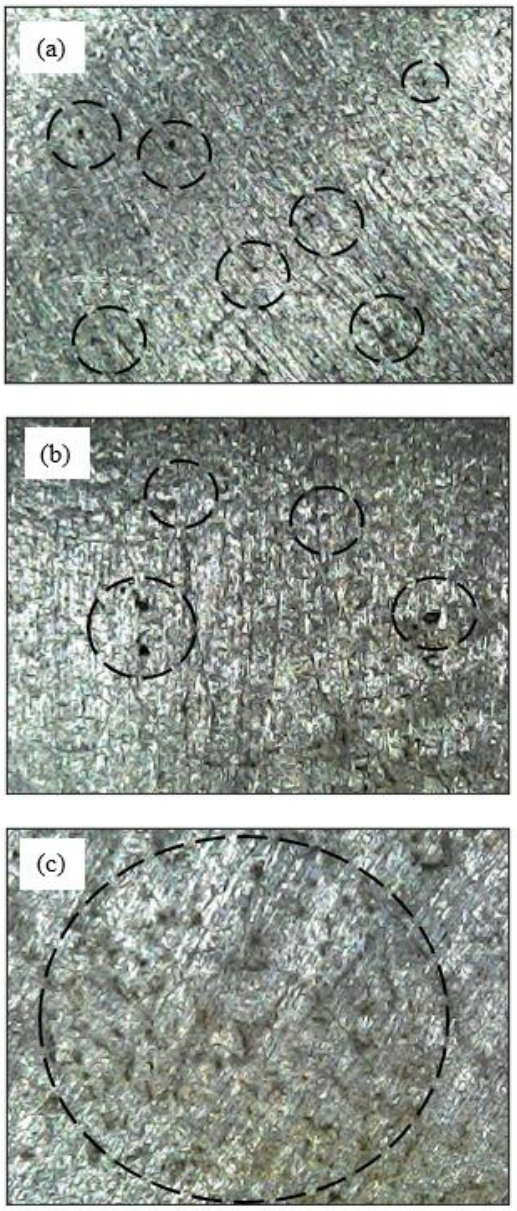

Figure 5 Optical microscope photos of the electrode surface after the potentiodynamic polarisation test at a magnification of 500 x for (a) WSC, (b) CMS and (c) CPI electrodes

The pure iron electrode (CPI) revealed irregular small-size pits that were dispersed all over the surface, as can be seen in Figure 5 (c), which was in agreement with a more negative E_{pit} value of CPI. Dura & Breslin (2019) reported similar findings, as pure iron demonstrated little evidence of large pits with uniform dissolution compared to stainless steel electrodes [18]. Meanwhile, the regular pitting of small size could be observed on the surface of WSC and CMS in Figure 5 (a) and (b), respectively. The similar type of pitting obtained on the surface of WSC and CMS might be attributed to the similar category of mild steel materials.

3.2 Dye Removal Performance by Different Fe-Based Electrodes

The effect of different Fe-based electrodes on the AR18 dye removal efficiency was further examined to correlate their surface characteristics and electrochemical behaviour with the removal performance via the EC process. Figure 6 displays the AR18 dye removal efficiency with time using WSC, CMS and CPI electrodes. The removal efficiency of WSC (99.7%) was found to be slightly higher than that of the commercial electrodes of CMS (98.7%) and CPI (98.1%).

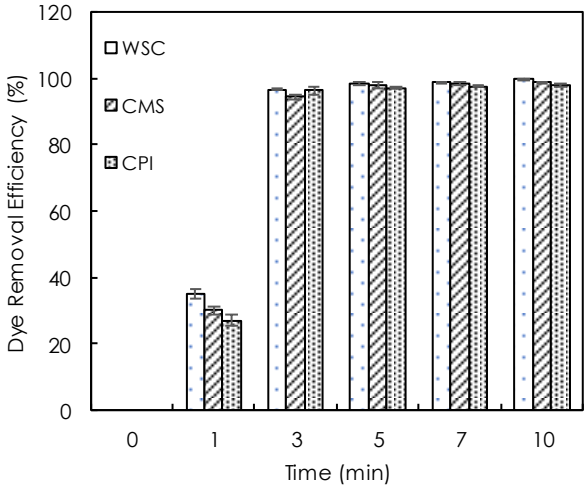

Figure 6 Removal efficiency of AR18 dye versus time using different Fe-based electrodes of WSC, CMS and CPI (Current density=25 mA/cm^2, initial dye concentration =100mg/L, pH=6.8 (original pH of dye), NaCl=2g/L and IED=0.5cm)

However, it can be concluded that all Fe-based electrodes performed an excellent removal efficiency performance, indicating that the different purity, composition and electrochemical behaviour of Fe materials did not significantly influence the dye removal process during the EC treatment. Müller *et al.*, (2019) reported a similar observation, as the purity of the Fe anodes (99% and 92% of Fe composition) used in their work did not substantially influence the long-term performance of the electrodes [33]. Their results showed almost identical faradaic efficiency behaviour, surface layer growth mineralogy and total cell potential. Since electrode purity did not appear to be a critical factor in the performance of the EC-Fe system, this finding suggests that more affordable and

readily accessible lower-purity electrode materials like WSC could be employed without diminishing its long-term efficiency.

Meanwhile, the remaining Fe ions concentration in the treated water using different types of Fe-based electrodes was also examined, and the findings are shown in Table 2. All types of Fe-based electrodes revealed that Fe ions were not detected in the treated water after the EC process. This was due to the Fe ions released from the anode being actively coagulated with the pollutants during the EC process and consequently removed through sedimentation or floatation of flocs [34].

Table 2 The amount of Fe ions present in the treated water and the permissible Fe ion limit specified in the Environmental Quality (Industrial Effluent) Regulation 2009 [35]

Electrode material	Treated water [Fe^{3+}] (ppm)	Standard A [Fe^{3+}] (ppm)	Standard B [Fe^{3+}] (ppm)
WSC	*N.D<0.02		
CMS	*N.D<0.02	1.0	5.0
CPI	*N.D<0.02		

- N.D is not detected

Moreover, the energy consumption of the WSC was found to be slightly higher but still comparable with the CMS and CPI (Table 3), which was in agreement with the passivation behaviour of the WSC, as discussed previously. Meanwhile, the consumption of the electrode for all the Fe-based electrodes during the EC process was found to be almost similar at a constant current density. The operating costs for the EC process using WSC, CMS, and CPI were found to be comparable, in the range of RM2.36 to RM2.47/m^3. Therefore, it could be concluded that WSC was an efficient, low cost and harmless electrode [36]. The WSC electrodes could also be beneficially used as an alternative to the commercial Fe-based electrodes in the EC process to treat dye-containing wastewater.

Table 3 Performance of different Fe-based electrodes for AR18 dye removal by EC process

Electrode materials	Percentage removal (%)	Voltage required (V)	Energy Consumption (kWh/m^3)	Electrode Consumption (kg/m^3)	Operating cost (RM/m^3)
WSC	99.7	6.5	2.84	0.046	2.36
CMS	98.7	5.5	2.46	0.047	2.39
CPI	98.1	6.0	2.69	0.047	2.47

4.0 CONCLUSION

In this study, WSC demonstrated an excellent potential electrode as an alternative to the commercial ones for the EC process. From the electrochemical behaviour study, the corrosion potential (E_{corr}) of WSC was found to be more negative (-0.954 V vs. SCE) compared to CPI (-0.947 V vs. SCE) and CMS (-0.908 V vs. SCE), indicating a slightly higher Fe ion dissolution in WSC electrodes. This aligns with its EC performance, where WSC achieved a removal efficiency of 99.7%, slightly higher than CMS (98.7%) and CPI (98.1%). However, the application of WSC electrodes required a slightly higher voltage to produce an equivalent current density as the commercial electrodes. Thus, to reduce energy consumption, a parameter effects study is required to identify the optimal operating conditions for WSC electrodes in the removal of AR18 dye using the EC process.

Acknowledgement

The authors gratefully acknowledge the financial support received from Universiti Teknologi MARA (MyRA Lepasan PhD Grant, 600-RMC/GPM LPHD 5/3 (068/2023)), Universiti Teknologi MARA, Cawangan Pulau Pinang, as well as Universiti Sains Malaysia for providing laboratory facilities throughout this research work.

Conflicts of Interest

The author(s) declare(s) that there is no conflict of interest regarding the publication of this paper.

References

[1] Samsami, S., Mohamadi, M., Sarrafzadeh, M. H., Rene, E. R. and Firoozbahr, M. 2020. Recent Advances in the Treatment of Dye-Containing Wastewater from Textile Industries: Overview and Perspectives. *Process Safety and Environmental Protection*. 143: 138–163. Doi: https://doi.org/10.1016/j.psep.2020.05.034.

[2] Handayani, W., Kristijanto, A. I. and Hunga, A. I. R. 2018. Are Natural Dyes Eco-Friendly? A Case Study on Water Usage and Wastewater Characteristics of Batik Production by Natural Dyes Application. *Sustainable Water Resources Management*. 4 (4): 1011–1021. Doi: https://doi.org/10.1007/s40899-018-0217-9.

[3] Khosravi, R., Hazrati, S. and Fazlzadeh, M. 2015. Decolorization of AR18 Dye Solution by Electrocoagulation: Sludge Production and Electrode Loss in Different Current Densities. *Desalination and Water Treatment*. 57 (31): 1–9. Doi: https://doi.org/10.1080/19443994.2015.1063092.

[4] Ghalwa, N. M. A., Saqer, A. M. and Farhat, N. B. 2016. Removal of Reactive Red 24 Dye by Clean Electrocoagulation Process using Iron and Aluminum Electrodes. *Journal of Chemical Engineering & Process Technology*. 7(1): 1–7. Doi: https://doi.org/10.4172/2157-7048.1000269.

[5] Akhtar, A., Aslam, Z., Asghar, A., Bello, M. M. and Raman, A. A. A. 2020. Electrocoagulation of Congo Red Dye-Containing Wastewater: Optimization of Operational Parameters and Process Mechanism. *Journal of Environmental Chemical Engineering*. 8: 104055. Doi: https://doi.org/10.1016/j.jece.2020.104055.

[6] Camcioglu, S., Ozyurt, B. and Hapoglu, H. 2017. Effect of Process Control on Optimization of Pulp and Paper Mill Wastewater Treatment by Electrocoagulation. *Process Safety and Environmental Protection*. 111: 300–319. Doi: https://doi.org/10.1016/j.psep.2017.07.014.

[7] Bener, S., Bulca, Ö., Palas, B., Tekin, G., Atalay, S. A. and Ersöz, G. 2019. Electrocoagulation Process for the Treatment of Real Textile Wastewater: Effect of Operative Conditions on the Organic Carbon Removal and Kinetic Study. *Process Safety and Environmental Protection*.129: 47–54. Doi: https://doi.org/10.1016/j.psep.2019.06.010.
[8] Verma, A. K. 2017. Treatment of Textile Wastewaters by Electrocoagulation Employing Fe-Al Composite Electrode. *Journal of Water Process Engineering*. 20: 168–172. Doi: https://doi.org/10.1016/j.jwpe.2017.11.001.
[9] Khorram, A. G. and Fallah, N. 2018. Treatment of Textile Dyeing Factory Wastewater by Electrocoagulation with Low Sludge Settling Time : Optimization of Operating Parameters by RSM. *Journal of Environmental Chemical Engineering*. 6: 635–642. Doi: https://doi.org/10.1016/j.jece.2017.12.054.
[10] Azarian, G., Nematollahi, D., Rahmani, A. R., Godini, K., Bazdar, M. and Zolghadrnasab, H. 2014. Monopolar Electro-Coagulation Process for Azo Dye C.I. Acid Red 18 Removal from Aqueous Solutions. *Avicenna J Environ Health Eng*. 1(1): 1–6. Doi: https://doi.org/10.5812/ajehe.354.
(11) Elazzouzi, M., Haboubi, K., Elyoubi, M. S. and Kasmi, A. El. 2019. A Developed Low-Cost Electrocoagulation Process for Efficient Phosphate and COD Removals from Real Urban Wastewater. *ES Energy & Environment*. 5: 66–74. Doi: https://doi.org/10.30919/esee8c302.
[12] Soonsorn, C., Khuanmar, K., Padungthon, S. and Weerayutsil, P. 2018. Using Waste from Food Cans as Electrode in Electrocoagulation for Wastewater Treatment. *International Journal of Engineering & Technology*. 7(4.38): 1372–1375. Doi: https://doi.org/10.14419/ijet.v7i4.38.27877.
[13] Bakshi, A., Verma, A. K. and Dash, A. K. 2020. Electrocoagulation for Removal of Phosphate from Aqueous Solution : Statistical Modeling and Techno-Economic Study. *Journal of Cleaner Production*. 246: 118988. Doi: https://doi.org/10.1016/j.jclepro.2019.118988.
[14] Nippatla, N. and Philip, L. 2020. Electrochemical Process Employing Scrap Metal Waste as Electrodes for Dye Removal. *Journal of Environmental Management*. 273: 111039. Doi: https://doi.org/10.1016/j.jenvman.2020.111039.
[15] Bani-Melhem, K., Al-Kilani, M.R. and Tawalbeh, M. 2023. Evaluation of Scrap Metallic Waste Electrode Materials for the Application in Electrocoagulation Treatment of Wastewater. *Chemosphere*. 310: 136668. Doi : https://doi.org/10.1016/j.chemosphere.2022.136668.
[16] Hashem, S. A. M., Gaber, G. A., Hussein, W. A. and Ahmed, A. S. I. 2024. Electrocoagulation Process with Fe/Al Electrodes to Eliminate Pollutants from Real and Synthetic Wastewater. *Results in Materials*. 23: 100606. Doi: https://doi.org/10.1016/j.rinma.2024.100606.
[17] Bani-Melhem, K. and Rasool Al-Kilani, M. 2023. A Comparison between Iron and Mild Steel Electrodes for the Treatment of Highly Loaded Grey Water using an Electrocoagulation Technique. *Arabian Journal of Chemistry*. 16: 105199. Doi: https://doi.org/10.1016/j.arabjc.2023.105199.
[18] Dura, A. and Breslin, C. B. 2019. Electrocoagulation using Stainless Steel Anodes : Simultaneous Removal of Phosphates, Orange II and Zinc Ions. *Journal of Hazardous Materials*. 374: 152–158. Doi: https://doi.org/10.1016/j.jhazmat.2019.04.032.
[19] Nurulhuda, A., Suzylawati, I., Farhan, A. S. and Zuhairi, A. A. 2021. Electrochemical Behaviors of Waste Steel Container as Electrodes for Removal of Acid Red 18 Dye in Water through Electrocoagulation Process. *Desalination and Water Treatment*. 230: 331–345. Doi: https://doi.org/10.5004/dwt.2021.27432.
[20] Azo Materials, AISI 1018 Mild/Low Carbon Steel, 2019. https://www.azom.com/article.aspx?ArticleID=6115 (accessed March 3, 2021).
[21] Yu, Y., Zhong, Y., Wang, M. and Guo, Z. 2021. Electrochemical Behavior of Aluminium Anode in Super-Gravity Field and Its Application in Copper Removal from Wastewater by Electrocoagulation. *Chemosphere*. 272: 129614. Doi: https://doi.org/10.1016/j.chemosphere.2021.129614.
[22] Dura, A. 2013. Electrocoagulation for Water Treatment: The Removal of Pollutants Using Aluminium Alloys, Stainless Steels and Iron Anodes, National University of Ireland Maynooth. http://eprints.maynoothuniversity.ie/6744/1/adelaide-dura.pdf.
[23] Ryan, D. R., McNamara, P. J., Baldus, C. K., Wang, Y. and Mayer, B. K. 2023. Peroxi-Electrocoagulation for Treatment of Trace Organic Compounds and Natural Organic Matter at Neutral pH. *Environmental Science: Advances*. 2: 1574–1586. Doi: https://doi.org/10.1039/d3va00138e.
[24] Shaker, O. A., Safwat, S. M. and Matta, M. E. 2023. Nickel Removal from Wastewater using Electrocoagulation Process with Zinc Electrodes under Various Operating Conditions: Performance Investigation, Mechanism Exploration, and Cost Analysis. *Environmental Science and Pollution Research*. 30: 26650–26662. Doi: https://doi.org/10.1007/s11356-022-24101-6.
[25] Bazrafshan, E., Moein, H., Mostafapour, F. K. and Nakhaie, S. 2013. Application of Electrocoagulation Process for Dairy Wastewater Treatment. *Journal of Chemistry*. 2013: 1–8. Doi: https://doi.org/10.1155/2013/640139.
[26] Abfertiawan, M. S., Syafila, M., Handajani, M., Hasan, F., Oktaviani, H., Gunawan, F. and Djali, dan. F. 2024. Batch Electrocoagulation Process for the Removal of High Colloidal Clay from Open-Cast Coal Mine Water Using Al and Fe Electrodes. *Mine Water and the Environment*. 43: 516–528. Doi: https://doi.org/10.1007/s10230-024-01004-1.
[27] Sakthisharmila, P., Palanisamy, P. N. and Manikandan, P. 2018. Removal of Benzidine Based Textile Dye using Different Metal Hydroxides Generated in Situ Electrochemical Treatment-A Comparative Study. *Journal of Cleaner Production*. 172: 2206–2215. Doi: https://doi.org/10.1016/j.jclepro.2017.11.192.
[28] Tenaga Nasional Berhad Malaysia. Pricing & Tariffs https://www.tnb.com.my/commercial-industrial/pricing tariffs1/ (accessed Jan 19, 2021).
[29] The London Metal Exchange. London Metal Exchange https://www.lme.com/en-GB/Metals/Non ferrous#tabIndex=0 (accessed Jan 19, 2021).
[30] Qingli Sdn. Bhd. Malaysia. http://www.foodbizmalaysia.com/company/details/50001 669/syarikat-qingli-sdn-bhd (accessed Jan 19, 2021).
[31] Alessandro Pirolini. Galvanic Corrosion of Steel and Other Metals https://www.azom.com/article.aspx?ArticleID=11833 (accessed Aug 29, 2021).
[32] Schweitzer, P. A. 2010. Fundamentals of Corrosion; Taylor & Francis Group: New York, Doi: https://doi.org/10.1002/j.15518833.1941.tb19650. x.
[33] Müller, S., Behrends, T. and Genuchten, C. M. Van. 2019. Sustaining Efficient Production of Aqueous Iron during Repeated Operation of Fe(0)-Electrocoagulation. *Water Research*. 155: 455–464. Doi: https://doi.org/10.1016/j.watres.2018.11.060.
[34] Nasrullah, M., Zularisam, A. W., Krishnan, S., Sakinah, M., Singh, L. and Fen, Y. W. 2019. High Performance Electrocoagulation Process in Treating Palm Oil Mill Effluent using High Current Intensity Application. *Chinese Journal of Chemical Engineering*. 27 (1): 208–217. Doi: https://doi.org/10.1016/j.cjche.2018.07.021.
[35] Department of Environmental Malaysia. Environmental Quality Industrial Effluent Regulations 2009 - _P.U.A_434-2009.Pdf. Percetakan Nasional Malaysia Berhad. 2009.
[36] Chafi, M., Gourich, B., Essadki, A. H., Vial, C. and Fabregat, A. 2011. Comparison of Electrocoagulation using Iron and Aluminium Electrodes with Chemical Coagulation for the Removal of a Highly Soluble Acid Dye. *Desalination*. 281: 285–292. Doi: https://doi.org/10.1016/j.desal.2011.08.004.